MATH 723 Mathematical Neuroscience Spring 2008
Instructor: Georgi Medvedev

2 Lecture 2. Approximate systems.

2.1 Reduction of the HH model to a $2D$ system.

The original HH system consists of 4 differential equations. In the present lecture, we introduce several approximations which allow to reduce the HH model to a system of 2 differential equations. The analysis of the approximate $2D$ model provides an insight into the mechanism for spike generation in the HH model. The following observations lead to the desired reduction:

Step 1. Note that $\tau_m(V) \ll \tau_h(V)$,$\tau_n(V)$ (see Figure 1.2),i.e., the dynamics of the activation of the sodium current has the fastest time scale. Therefore, to leading order, we approximate $m(t)$ by its steady state value: $m \approx m_\infty(V)$. The resulting system has the following form:

$$\dot{V} = -g_{Na}m_\infty^3(V)h(V-E_{Na}) - g_K n^4(V-E_K) - g_L(V-E_L) + I, \tag{2.1}$$

$$\dot{n} = \frac{n_\infty(V)-n}{\tau_n(V)}, \tag{2.2}$$

$$\dot{h} = \frac{h_\infty(V)-h}{\tau_h(V)}. \tag{2.3}$$

Step 2. The following observation is due to Krinsky and Kokoz [KK]. The dynamics of h is similar to that of n. The numerics in Figure 2.1 show after a short period of time necessary for transients to settle down, $h+n \approx 1$. More precisely, $1.1n + h \approx 0.89$ (see Figure 2.1).

By approximating $h \approx l(n), l(n) = 0.89 - 1.1n$, we arrive at the following system of two differential equations:

$$\dot{V} = -g_{Na}m_\infty^3(V)l(n)\,(V-E_{Na}) - g_K n^4\,(V-E_K) - g_L\,(V-E_L) + I, \tag{2.4}$$

$$\dot{n} = \frac{n_\infty(V)-n}{\tau_n(V)}, \tag{2.5}$$

Step 3. Finally, it is convenient to approximate steady-state functions $m_\infty(v)$ and $n_\infty(v)$ and time constant $\tau_n(v)$ using hyperbolic functions [BRS]:

$$s_\infty(V) = \left\{1+\exp\left(\frac{V-\theta_s}{\sigma_s}\right)\right\}^{-1},\ s=m,n, \tag{2.6}$$

$$\tau_n(V) = \bar{\tau}_n \cosh\left(\frac{V-\theta_n}{2\sigma_n}\right), \tag{2.7}$$

The original functions and their approximations (2.6) and (2.7) are shown in Figure 2.2a. The parameter values for the reduced model (2.4) and (2.5) are summarized in

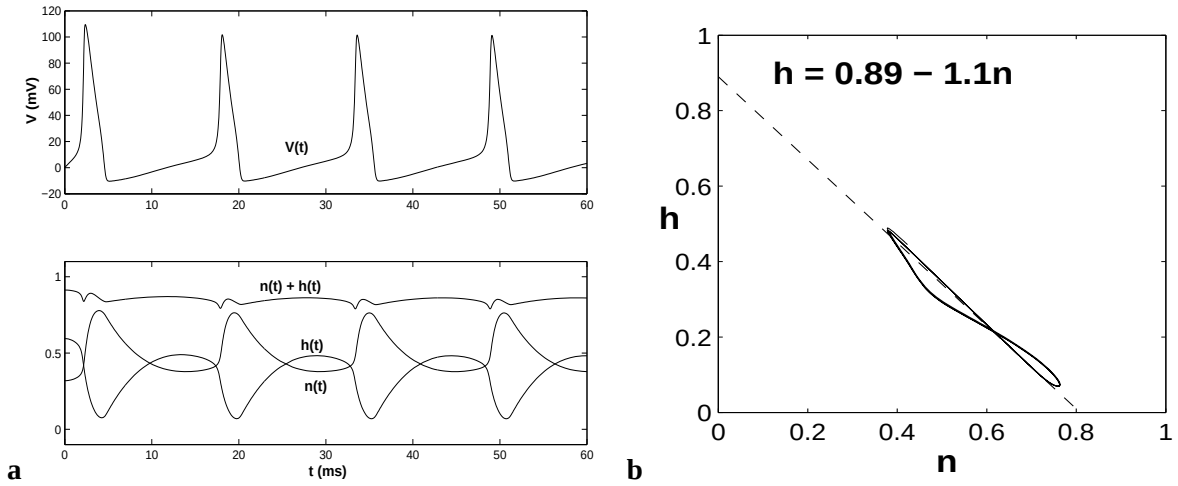

Figure 2.1: Plots in **a** and **b** show that variables n and h are approximately linearly dependent.

Table 2.

g_{Na}	$120mS/cm^2$	E_{Na}	$120mV$	θ_m	$25mV$	σ_m	-9.5
g_K	$36mS/cm^2$	E_K	$-12mV$	θ_n	$11.3mV$	σ_n	-19.5
$\bar{\tau}_n$	21	g_L	$0.3mS/cm^2$	E_L	$10.6mV$	C	$1\mu F/cm^2$

2.2 The rescaled system.

Variables v and n in the reduced HH model have different models of magnitude. During an AP, voltage varies from -20mV to about 100mV, while the values of the gating variable range from 0.4 to 1. To analyze (2.4) and (2.5), it is convenient to rescale the dynamical variables so that they have the same orders of magnitude:

$$V = k_V v,\ k_V = 100mV,\ \tau = k_t t,\ k_t = 1ms. \tag{2.8}$$

We also rescale the maximal conductances and the reversal potentials:

$$g_s = \tilde{g}_s \times 100mScm^{-2} \text{ and } E_s = \tilde{E}_s \cdot k_v, \quad s = \{m, n\}.$$

Thus, we obtain the following nondimensional system:

$$\epsilon \dot{v} = -\tilde{g}_{Na} m_\infty^3(v) h (v - \tilde{E}_{Na}) - \tilde{g}_K n^4 (v - \tilde{E}_K) - \tilde{g}_L (v - \tilde{E}_L) + \tilde{I},, \tag{2.9}$$

$$\dot{n} = \frac{\tilde{n}_\infty(v) - n}{\tilde{\tau}_n(v)}. \tag{2.10}$$

where $\tilde{s}_\infty(v) = s_\infty(k_V v),\ s = \{m, n\}$ and $\tilde{\tau}_n(v) = \tau_n(k_V v)$. The derivative of v is multiplied by a small nondimensional parameter $\epsilon = 10^{-2}$. This indicates that that the dynamics of v and n have different timescales. Equations (2.10) and (2.10) imply that typically: $\dot{v} = O\left(\epsilon^{-1}\right)$ while $\dot{n} = O(1)$, i.e., v changes

a

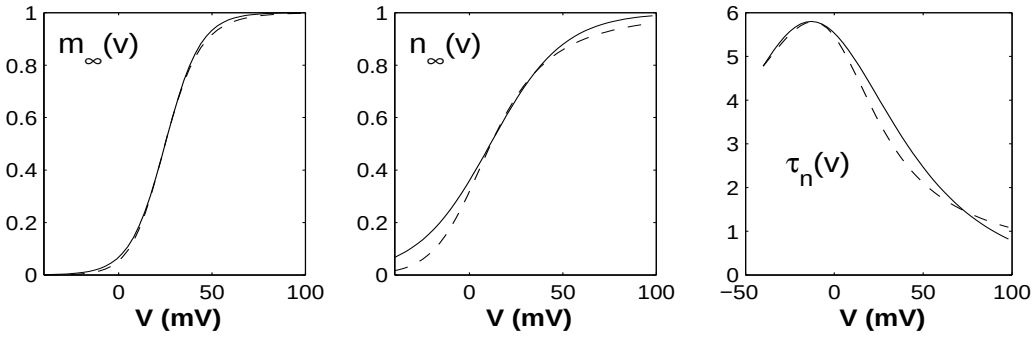

b

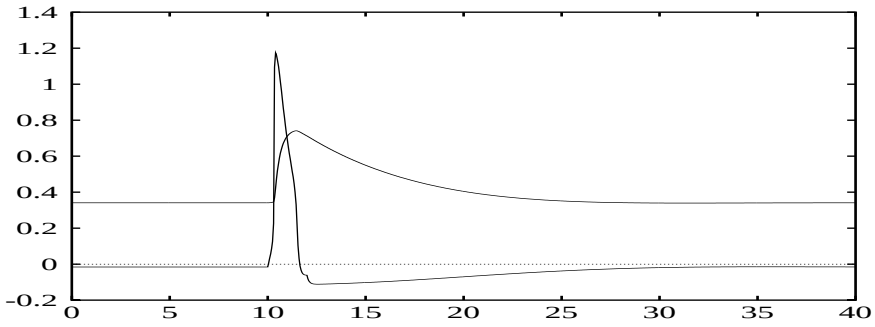

Figure 2.2: **a.** Steady-state functions $m_\infty(v)$ and $n_\infty(c)$, and and time constant $\tau_n(v)$ (solid line) and their approximations by the hyperbolic functions (dashed line). **b.** Action potential generated by the $2D$ approximation of the HH model by applying a step current pulse.

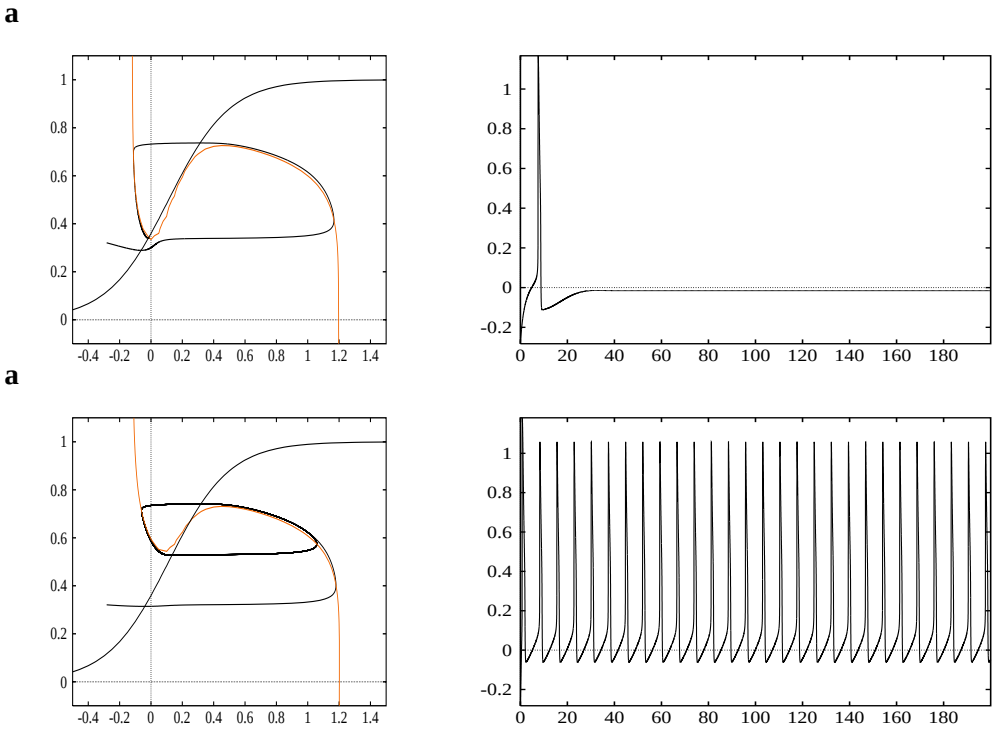

Figure 2.3: The rescaled system: the phase plane and time series: a) excitable regime and b) oscillating regime.

much faster than n. For this reason, v is called a *fast* variable. The $v-$time series in Figure 2.3 show alternating intervals of fast and slow dynamics. Systems of ODEs with small parameters multiplying time-derivatives in some of the equations are called *singularly perturbed* or *fast-slow* systems. In the following subsection, we describe a geometric method for analyzing a 2D singularly perturbed system.

2.3 The FitzHugh-Nagumo model: slow-decomposition decomposition

Below we outline some ideas used for analyzing singularly perturbed systems of ODEs. To make our discussion more explicit, we will use a specific example of a $2D$ singularly perturbed system, the FitzHugh-Nagumo model:

$$\epsilon \dot{v} = f(v) - n + I, \tag{2.11}$$

$$\dot{n} = v - \gamma n, \tag{2.12}$$

where v and n are the dynamical variables, and $I, \gamma > 0, 0 < \epsilon \ll 1$ are parameters. A smooth function $f(v)$ is qualitatively cubic, i.e. it has two extrema and $\lim_{v \to \pm} f(v) = \pm\infty$. A small parameter $\epsilon > 0$ is called a

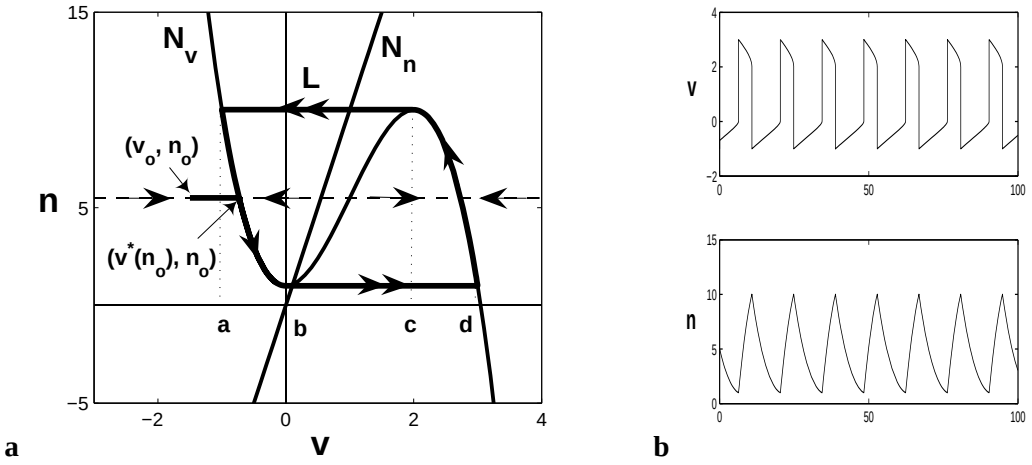

Figure 2.4: The FitzHugh-Nagumo model: **a**. The phase plane, **b**. Solution plots.

relaxation parameter. Along with (2.11)-(2.12), we shall consider the following system of equations:

$$\frac{dv}{d\tau} = f(v) - n + I, \tag{2.13}$$

$$\frac{dn}{d\tau} = \epsilon(v - \gamma n), \tag{2.14}$$

where $\tau = \epsilon^{-1}t$ is called the fast time. By formally taking the limit as $\epsilon \to 0$ in (2.13) and (2.14) we arrive at the fast subsystem:

$$\frac{d\tilde{v}}{d\tau} = f(\tilde{v}) - \tilde{n} + I, \tag{2.15}$$

$$\frac{d\tilde{n}}{d\tau} = 0. \tag{2.16}$$

Let (v_0, n_0) be the initial condition for (2.15), (2.16), as shown in Fig 2.3. For almost all initial conditions (v_0, n_0), v_0 belongs to the domain of attraction of one of the stable fixed points of the $1D$ ODE:

$$\frac{d\tilde{v}}{d\tau} = f(\tilde{v}) - n_0 + I.$$

Denote this fixed point by $v^*(n_0)$. The trajectory of the fast system (2.15), (2.16) starting at (v_0, n_0) tends to $(v^*(n_0), n_0)$ as $\tau \to \infty$ along the line $n = n_0$ (see Figure 2.4). The vector field generated by (2.15),(2.16) is called the *fast* vector field. The theory for *singularly perturbed* systems implies that for sufficiently small $\epsilon > 0$, the solutions of the fast system (2.15) and (2.16) approximate those of the original system (2.13) and (2.14) with the (same initial condition) up to the time when the trajectory of the fast system enters some $O(\epsilon)$ neighborhood of $(v^*(n_0), n_0)$. To study the dynamics of (2.13) and (2.14) after that moment of time, we consider original system (2.11), and (2.12). Again, by formally taking the limit as $\epsilon \to 0$, from (2.13) and (2.14) we derive the *slow* system:

$$n = f(v) + I, \tag{2.17}$$

$$\dot{n} = v - \gamma n, \tag{2.18}$$

The dynamics of the slow system is constrained by the two outer (stable) branches of the slow curve

$$n = f(v) + I.$$

The set of points with coordinates satisfying (2.17) is also called the $v - nullcline$: $N = \{(v, n) : n = f(v) + I\}$ (see Figure 2.4). The motion along N is determined by the equation (2.18). By differentiating both sides of (2.17) with respect to time and by combining the result with (2.18), we obtain:

$$f'(v)\frac{dv}{dt} = v - \gamma n, \tag{2.19}$$

By plugging in (2.17) into (2.19) we obtain

$$\frac{dv}{dt} = \frac{v - \gamma(f(v) + I)}{f'(v)}, \tag{2.20}$$

Equation (2.20) is valid outside of some neighborhoods of the points of extrema of $f(v)$ where $f'(v) = 0$. According to (2.20) on the slow manifold trajectory with initial condition, as shown in Figure 2.4, will move down along the left hand outer branch of N_v until it reaches an $O(\epsilon)$ neighborhood of a. After that the point will 'jump' to the opposite stable branch of N_v under the action of the fast vector field. The description of the slow dynamics along this branch is completely analogous to that for the left outer branch. Therefore, after some finite time the phase trajectory remains in the neighborhood of the closed curve L composed of the segments of the slow manifold joined by horizontal segments (see Figure 2.4a). L is called a relaxation limit cycle. The alternation of the slow motions and fast jumps generates relaxation oscillations (see Figure 2.4b). The above discussion shows that for a $2D$ singularly perturbed systems such as (2.13) and (2.14), the phase plane is to a large extent is determined by the geometries of the $v-$ and $n-$ nullclines:

$$n = f(v) + I \text{ and } n = \frac{1}{\gamma}v.$$

In the FHN model, parameter I plays the same role as the applied current in the HH model. Let us consider how the variation of I affects the qualitative dynamics of the FHN model. Note that changing I results in the translation of the voltage nullcline in the vertical direction. In particular, by decreasing I we can achieve that the point of the intersection of the two nullclines $(\bar{v}, \bar{n})$ lies on the left outer branch of L (see Figure 2.4).

Note that at $(v, n) = (\bar{v}, \bar{n})$ the right-hand side of (2.11) and (2.12) are zero. Therefore, $(\bar{v}, \bar{n})$ is a steady state or a fixed point. For the FHN, if the fixed point is located on the stable branch of the slow curve it attracts the trajectories following it. Therefore, after a finite time the dynamics of the system approaches the steady state $(\bar{v}, \bar{n})$. The phase plane discussion for the FHN system gives us a first insight into the mechanism of the excitation in the HH system. By changing the applied current in the HH system, we change the character of the fixed (it ceases to be attracting) and create an attracting limit cycle similar to L in the present example.

2.4 Two types of neuronal excitability

We conclude this lecture with an introductory discussion of the two major mechanisms for neuronal excitability (cf. [RE]). For this, we will use the phase plane techniques outlined in the present section. In

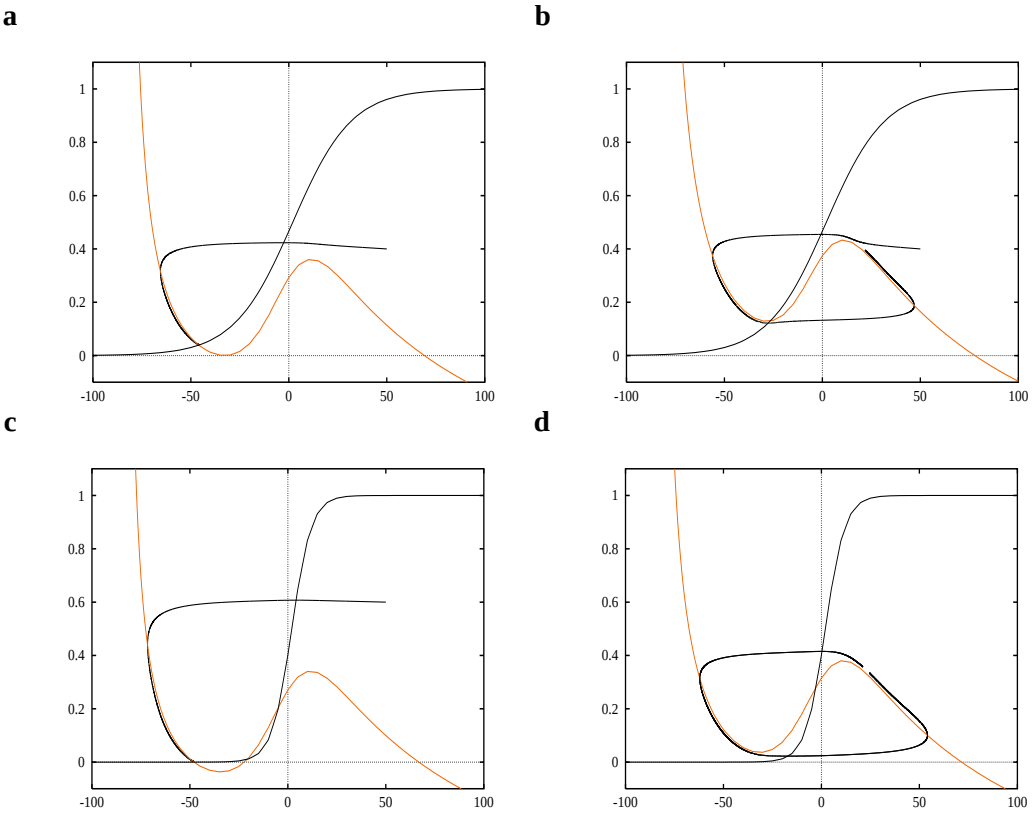

Figure 2.5: Phase portraits plotted for the ML model with different parameter values, illustrating two mechanisms of excitability: (a,b) Type II, (c,d) Type I.

the previous subsection, we showed that by changing the value of the applied current, I, one can affect the position of the fixed point in the FH system. The fixed point moves from the left branch to the middle branch of the cubic nullcline under the increase in I. For low values of I, the fixed point lies on the left branch and it blocks the motion of the trajectories along the slow manifold. Shortly after the fixed point passes the lower fold of N_v under the variation of I, it opens the way for the trajectories starting near the left branch to jump toward the right branch and gives rise to a limit cycle. This is an example of an excitable system, i.e., a system where a significant deviation from a stable steady state can be induced by a relatively small change of a control parameter. A similar mechanism is responsible for generation of the AP in the reduced HH system (Fig. 2.5a,b).

Next we discuss a different excitability mechanism illustrated in Fig. 2.5c,d. As in the previous case, the system shown in Fig. 2.6c is in an excitable state: the fixed point is lying on the left branch of the cubic nullcline. However, in contrast to the case discussed above, under the increase of applied current the fixed point collides with another one and disappears (Fig. 2.5d). As a result the limit cycle is born. The representative time series corresponding the two scenarios of transition to spiking are shown in Fig. 2.7 and 2.7. Note that in Fig. 2.6, the frequency of oscillations just near the transition is extremely low. This turns out to be a distinctive feature of a broad class of models, Type I models. The FHN model and the

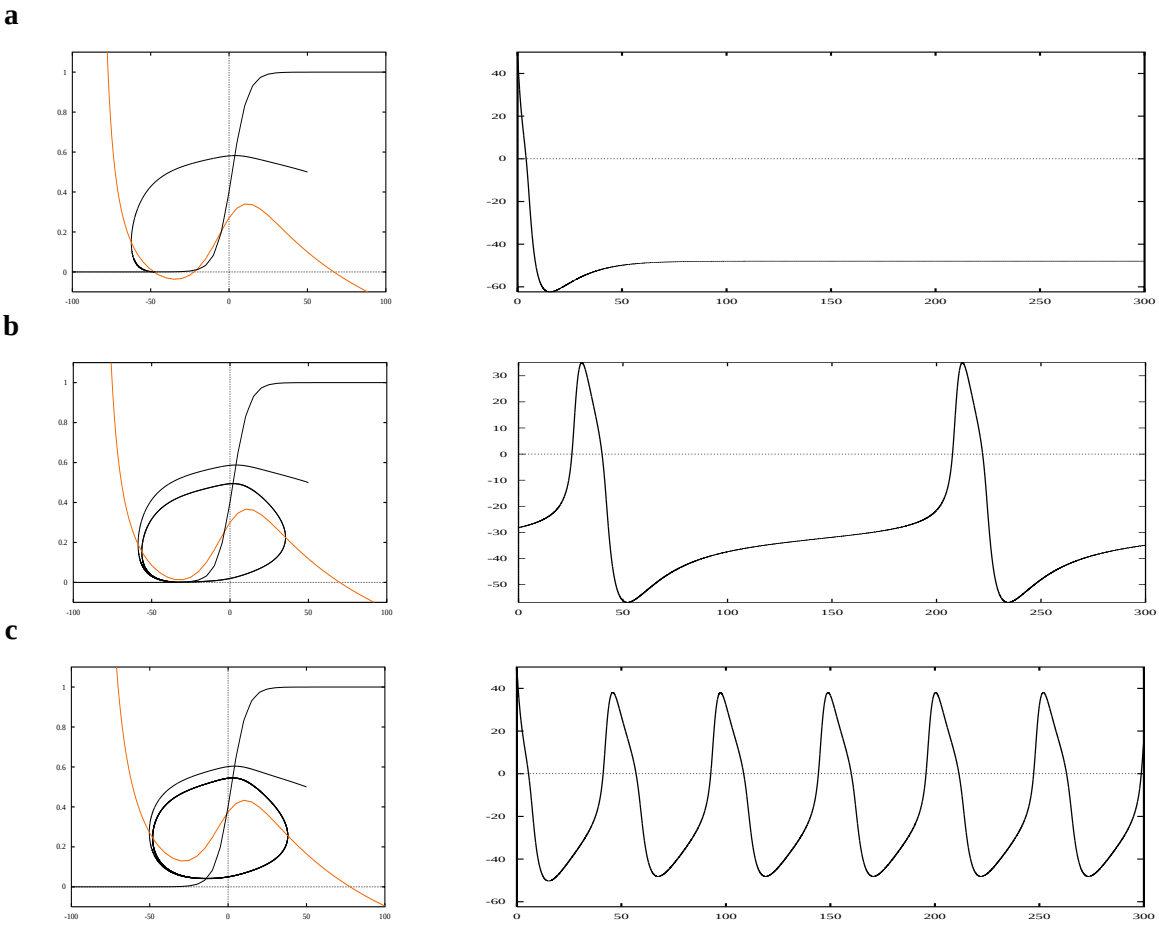

Figure 2.6: Phase portraits and the time series illustrating transition to spiking in Type I models.

reduced HH model belong to the Type II class of models. The frequency of oscillations is bounded from zero near the transition to spiking in Type II models. Explanation of these effects be given later after a brief introduction to elementary bifurcation theory in Lecture 4.

Homework project II.

a. Plot the phase portrait in the ML model. Determine whether it is a type I or type II model. Change the value(s) of some parameter(s) in this model to make it of a different type.

b. For the ML model in the Type II regime, use the phase plane analysis (along the lines of Section §2.3) to describe the mechanism of the AP generation under electrical stimulation. Derive the formula for the period of the relaxation limit cycle.

Bibliography

BRS R.J. Butera, J. Rinzel, J.C. Smith, *Models of Respiratory rhythm generation in the Pre-Botzinger*

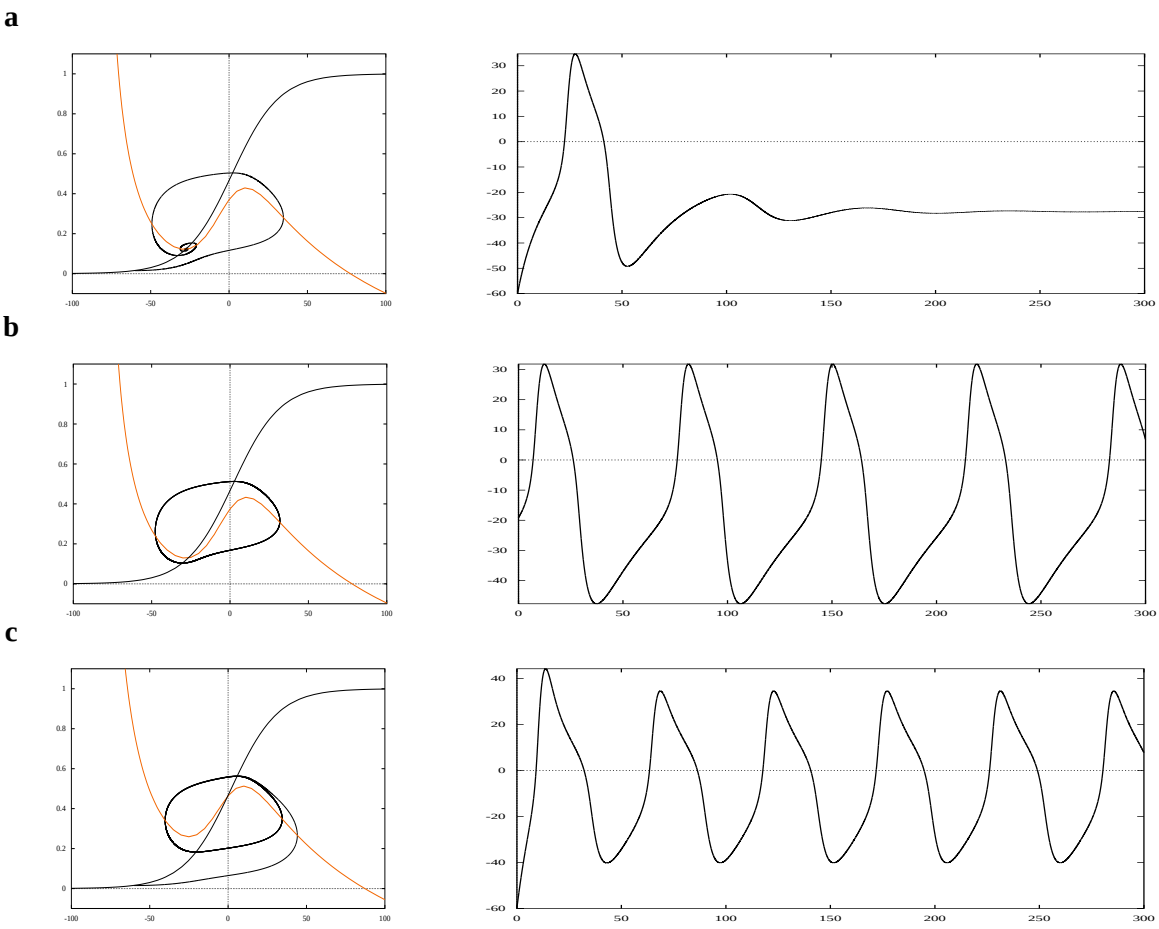

Figure 2.7: Phase portraits and the time series illustrating transition to spiking in Type II models.

Complex: I. Bursting pacemaker neurons, J. of Neurophys. **81**: 382-397, 1999)

KK VI Krinsky and YM Kokoz, Analysis of equations of excitable membranes I. Reduction of the Hodgkin-Huxley equations to a second order system. Biofizika, $18, 506-511, 1973$.

MKKR E.F. Mishchenko, Yu.S. Kolesov, A.Yu. Kolesov, and N.Kh. Rozov, *Asymptotic Methods in Singularly perturbed Systems*, Consultants Bureau, New York, 1994.

RE J. Rinzel and G.B. Ermentrout, Analysis of neural excitability and oscillations, in C. Koch and I. Segev, eds *Methods in Neuronal Modeling*, MIT Press, Cambridge, MA, 1989.